Front. Energy 2014, 8(3): 371–378
DOI 10.1007/s11708-014-0318-6

RESEARCH ARTICLE

Azzouz TAMAARAT, Abdelhamid BENAKCHA

Performance of PI controller for control of active and reactive power in DFIG operating in a grid-connected variable speed wind energy conversion system

Abstract Due to several factors, wind energy becomes an essential type of electricity generation. The share of this type of energy in the network is becoming increasingly important. The objective of this work is to present the modeling and control strategy of a grid connected wind power generation scheme using a doubly fed induction generator (DFIG) driven by the rotor. This paper is to present the complete modeling and simulation of a wind turbine driven DFIG in the second mode of operating (the wind turbine pitch control is deactivated). It will introduce the vector control, which makes it possible to control independently the active and reactive power exchanged between the stator of the generator and the grid, based on vector control concept (with stator flux or voltage orientation) with classical PI controllers. Various simulation tests are conducted to observe the system behavior and evaluate the performance of the control for some optimization criteria (energy efficiency and the robustness of the control). It is also interesting to play on the quality of electric power by controlling the reactive power exchanged with the grid, which will facilitate making a local correction of power factor.

Keywords wind power, doubly fed induction generator (DFIG), vector control, active power, reactive power, maximum power point tracking (MPPT)

1 Introduction

Wind energy is a source of energy used for centuries. Initially, this energy has been exploited in the mechanical fields. Subsequently, this type of energy is used to produce electricity. Wind systems integration within energy systems in terms of cost growth requires efficiency, namely the reduction of transaction costs and maintenance, and increasing the power captured from the wind. The use of the wind energy conversion system has been significantly expanding over the last few decades due to the fact that this energy source of production of electricity is emission free. The capacity of this energy in the world is estimated at over 160 GW [1].

For a variable-speed wind turbine, the generator is controlled by power electronic equipment. There are several reasons for using variable-speed operation of wind turbines, the possibilities to reduce stresses of the mechanical structure, acoustic noise reduction and the possibility to control active and reactive power [2].

The system studied in this paper consists of a three-bladed wind turbine, horizontal axis, connected to the network through a doubly fed induction generator (DFIG). The stator windings are connected directly to the network, while the rotor windings are supplied by a bi-directional power converter. Such machines may present some advantages in the field of production of variable-speed wind energy compared to other types of induction machines. This system has recently become very popular as a generator for variable-speed wind turbines mainly due to the fact that the power electronic converter only has to handle a fraction (about 20%–30%) of the total power [3], which is an economic interest in minimizing losses and the cost [4]. This cost depends on the size of frequency converters and their cooling systems. Another advantage of DFIG is increased power capture, which permits to conduct the speed wind turbine to the desired value which corresponds to the maximum power point tracking (MPPT). This may be done by changing the speed of the turbine in proportion to the change in wind speed. In addition, wind turbines based on the DFIG to control reactive power exchange with the network, and the

Received July 30, 2013; accepted September 6, 2013

Azzouz TAMAARAT (✉), Abdelhamid BENAKCHA
Laboratoire LGEB, Biskra University, Biskra City 07000, Algeria
E-mail: a.tamaarat@yahoo.fr

problem of reactive consumption power does not arise when using this type of generator. The aim of the control of the grid side converter is to maintain the DC-link capacitor voltage at a set value [5], it can be used for controlling reactive power flow between the grid and the grid side converter (the power factor is usually set to unity). The rotor-side converter is used to control the behavior of the machine in both sub- and super-synchronous modes as well as tracking the maximum power output characteristic of the wind turbine. The vector control for this converter ensures the decoupling control of stator active and reactive power drawn from the grid.

2 Wind turbine model

The wind recoverable energy P_w in the area swept by the propellers of a wind turbine is given by

$$P_w = \frac{1}{2}\rho A v_w^3, \quad (1)$$

where ρ is the air density, A is wind turbine blades swept area in the wind, and v_w is wind speed (in Fig. 1).

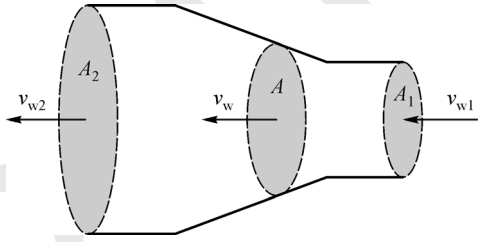

Fig. 1 Evolution of wind speed field in a wake

The aerodynamic efficiency of a wind turbine with horizontal axis is expressed by the power coefficient C_p. In 1919, Betz provided the theory of the wind turbine in which the maximum power coefficient is approximately 59% [6]. The maximum power coefficient is variable and depends on the characteristics of the turbine and the wind speed. It is often represented as a function of the tip speed ratio λ and the blade pitch angle β in a pitch-controlled wind turbine. λ, defined as the ratio of the tip speed of the turbine blades to wind speed, can be expressed as

$$\lambda = \frac{R\Omega_{turb}}{v_w},$$

where R is the blade radius and Ω_{turb} is the turbine rotor speed.

The output mechanical power of wind turbine is

$$p_v = \frac{1}{2}C_p\rho A v_w^3. \quad (2)$$

The power coefficient C_p can be approximated by mathematical Eq. (3) based on the modeling turbine characteristics as

$$C_p = \left[0.73\left(\frac{151}{\lambda'}\right) - 0.002\beta - 13.2\right]\exp\left(\frac{-18.4}{\lambda'}\right) \quad (3)$$

with

$$\lambda' = [1/(\lambda + 0.08\beta) - 0.035/(\beta^3 + 1)]^{-1}.$$

For different values β, the graph of C_p function λ is given below (in Fig. 2), which presents a maximum for a well-determined tip speed ratio, denoted by λ_{opt}.

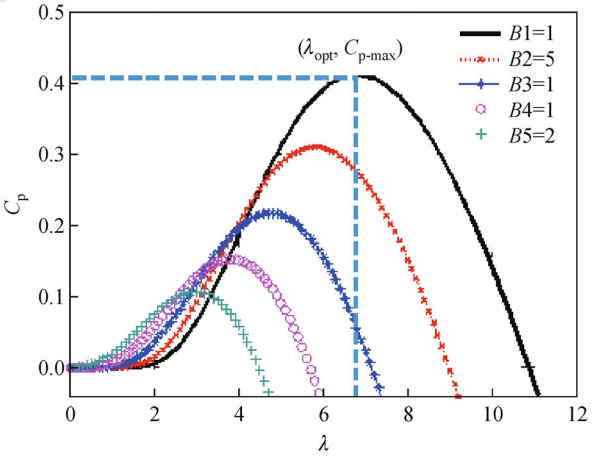

Fig. 2 Power coefficient C_p versus tip speed ratio λ

3 Optimal controller of a wind turbine

The objective of the control is to follow the maximum power curve between starting wind speed and rated wind speed (11.7 m/s). To extract the maximum power generated, the turbine rotates at the speed related to the optimal specific ratio λ_{opt} for which the power coefficient C_p is maximum (following the curve of the maximum power according to section AB, demonstrated in Fig. 3).

The turbine torque T_{turb} is the ratio of the output mechanical power to the shaft speed Ω_{turb}

$$T_{turb} = \frac{P_m}{\Omega_{turb}}.$$

The turbine is normally coupled to the generator shaft through a gearbox whose gear ratio k is chosen in order to set the generator shaft speed within a desired speed range. Neglecting the transmission losses, the torque T_g and shaft speed Ω_{mec} of the wind turbine, referred to the generator side of the gearbox, are given by

$$T_g = \frac{T_{turb}}{k} \text{ and } \Omega_{mec} = k\Omega_{turb}.$$

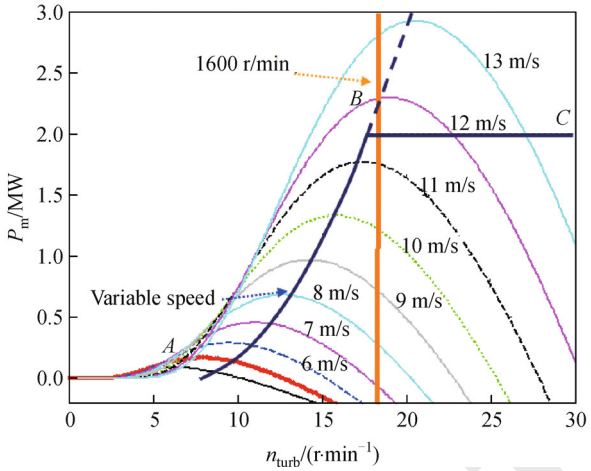

Fig. 3 Mechanical power depending on speed of wind turbine at different wind speeds

The system dynamics, neglecting the friction loss, is given by

$$J\frac{\mathrm{d}\Omega_{\mathrm{mec}}}{\mathrm{d}t} = T_{\mathrm{g}} - T_{\mathrm{em}}, \tag{4}$$

where J is the generator and the turbine moment of inertia and T_{em} is the electromagnetic torque.

To maximize the power extracted from the wind, the tip speed ratio should be kept around its optimal value λ_{opt}. The reference speed of the turbine $\Omega_{\mathrm{turb\text{-}ref}}$ can be deduced from the expression

$$\lambda_{\mathrm{opt}} = \frac{R\Omega_{\mathrm{turb\text{-}ref}}}{v_{\mathrm{w}}}.$$

The block diagram of the turbine model with the control of the speed is represented in Fig. 4. This model is expressed in Refs. [7–10]. The controller forces the rotor speed to track a desired speed reference signal chosen according to the fundamental operating modes.

The different configurations of variable speed wind turbines need power converter structures based on two AC-DC converters. Each converter needs active and reactive power control capability in order to extract the optimum power from the wind turbine while exchanging the appropriate reactive power with the power grid [11].

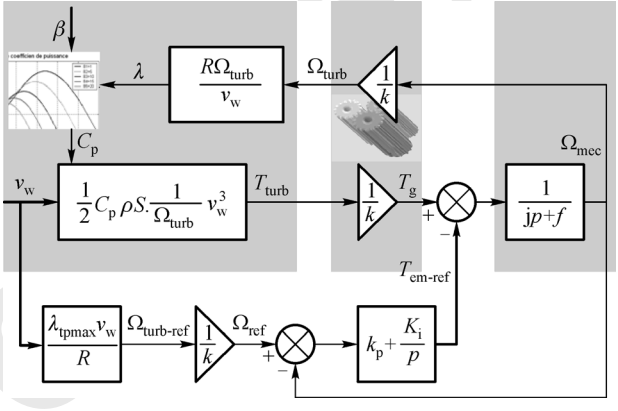

Fig. 4 Block diagram of speed control

4 DFIG model and control objectives

The electric and magnetic relationships governing the operation of the DFIG using Park Transformation is given by Eqs. (5) and (6) [12].

$$\begin{aligned} u_{sd} &= R_{\mathrm{s}}i_{sd} + \frac{\mathrm{d}\varphi_{sd}}{\mathrm{d}t} - \omega_{\mathrm{s}}\varphi_{sq}, \\ u_{sq} &= R_{\mathrm{s}}i_{sq} + \frac{\mathrm{d}\varphi_{sq}}{\mathrm{d}t} + \omega_{\mathrm{s}}\varphi_{sd}, \\ u_{\mathrm{r}d} &= R_{\mathrm{r}}i_{\mathrm{r}d} + \frac{\mathrm{d}\varphi_{\mathrm{r}d}}{\mathrm{d}t} - \omega_{\mathrm{r}}\varphi_{\mathrm{r}q}, \\ u_{\mathrm{r}q} &= R_{\mathrm{r}}i_{\mathrm{r}q} + \frac{\mathrm{d}\varphi_{\mathrm{r}q}}{\mathrm{d}t} + \omega_{\mathrm{r}}\varphi_{\mathrm{r}d}; \end{aligned} \tag{5}$$

$$\begin{aligned} \varphi_{sd} &= L_{\mathrm{s}}i_{sd} + Mi_{\mathrm{r}d}, \\ \varphi_{sq} &= L_{\mathrm{s}}i_{sq} + Mi_{\mathrm{r}q}, \\ \varphi_{\mathrm{r}d} &= L_{\mathrm{r}}i_{\mathrm{r}d} + Mi_{sd}, \\ \varphi_{\mathrm{r}q} &= L_{\mathrm{r}}i_{\mathrm{r}q} + Mi_{sq}; \end{aligned} \tag{6}$$

where R_{s}, R_{r}, L_{s} and L_{r} are the resistances and leakage inductances of the stator and rotor windings; M is the mutual inductance; u_{sd}, u_{sq}, $u_{\mathrm{r}d}$, $u_{\mathrm{r}q}$, i_{sd}, i_{sq}, $i_{\mathrm{r}d}$, $i_{\mathrm{r}q}$, l_{sd}, l_{sq}, $l_{\mathrm{r}d}$, $l_{\mathrm{r}q}$, φ_{sd}, φ_{sq}, $\varphi_{\mathrm{r}d}$ and $\varphi_{\mathrm{r}q}$ are the d and q components of the space vectors of stator and rotor voltages, currents, and fluxes. ω_{s} and ω_{r} are the angular frequencies of stator and rotor currents.

5 Vector control and control strategy

To achieve an independent control of the active and reactive power, the equations between the powers and rotor variables of the DFIG were established [13]. The vector control strategy based on proportional-integral (PI) controllers was proposed and widely used in the industry [14].

If the per phase stator resistance is neglected, which is a realistic approximation for medium and high power machines used in wind energy conversion, the stator voltage vector is consequently in quadrature advance in comparison with the stator flux vector [15]: $\varphi_{sd} = \varphi_{\mathrm{s}}$ and $\varphi_{sq} = 0$. In the stator voltage oriented reference frame, the d-axis is aligned with the supply voltage phasor u_{s}, and then $u_{sd} = u_{\mathrm{s}} = \omega_{\mathrm{s}}\varphi_{sd}$ and $u_{sq} = 0$. Hence, the active and reactive powers (P_{s}, Q_{s}) exchanged between the stator of the DFIG and the grid can be written according to the rotor currents as

$$P_s = u_{sq} i_{sq} = -u_s \frac{L_m}{L_s} i_{rq},$$
$$Q_s = u_{sq} i_{sd} = \frac{u_s^2}{L_s \omega_s} - \frac{u_s L_m}{L_s} i_{rq}. \quad (7)$$

Rotor voltages can be expressed by

$$u_{rd} = R_r i_{rd} - g\omega_s \left(L_r - \frac{M^2}{L_s} \right) i_{rq},$$
$$u_{rq} = R_r i_{rq} + g\omega_s \left(L_r - \frac{M^2}{L_s} \right) i_{rd} + g \frac{M u_s}{L_s}, \quad (8)$$

where g is ω_r/ω_s. The resulting block diagram of the DFIG is presented in Fig. 5.

The direct control method is based on a direct control of the active and reactive powers of the DFIG, by comparing references and calculated values of active and reactive powers [10]. The machine side converter control diagram is depicted in Fig. 6.

An important feature of the vector-controlled DFIG is the possibility to achieve decoupled control of the stator side active and reactive power in both motor and generator applications. The quadratic component of the rotor u_{rq} controls the active power (the electromagnetic torque) and the direct component u_{rd} controls the reactive power exchanged between the stator and the network.

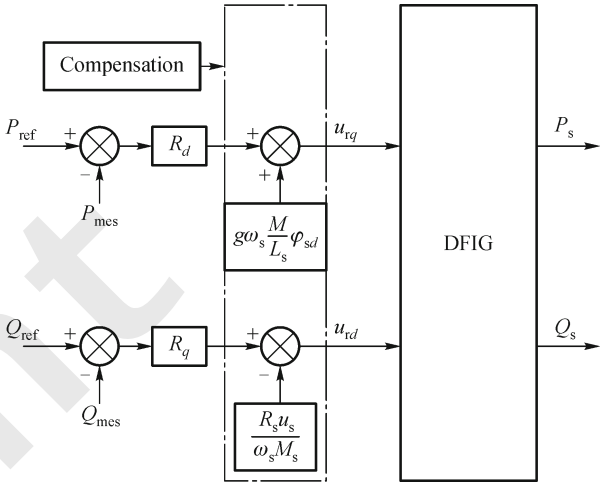

Fig. 6 Block diagram of DFIG power control (two PI controllers are used)

6 Simulation results

6.1 First case of simulation

Simulations are performed with a random wind speed, varying between 6 m/s and 8.5 m/s. A step is applied on the reactive power reference, from 0 kvar to 0.5 kvar, at t = 1.3 s, 0.5 kvar to 0.5 kvar, at t = 1.5 s and 0.5 kvar to 0 kvar, at t = 3.5 s.

Figure 7 shows, respectively, the wind gust (Fig. 7(a)), the power coefficient (Fig. 7(b)), the angular speed of the DFIG (Fig. 7(c)) and the mechanical power of wind turbine (Fig. 7(d)). The stator active and reactive power and its zoom are demonstrated in Figs. 8(a) and (b) according to the quadratic component of the rotor u_{rq} and the direct component u_{rd}. The rotor phase current and voltage according to the rotor speed changes are given in Fig. 9. On the other hand, Fig. 10 shows the variation of the stator phase current.

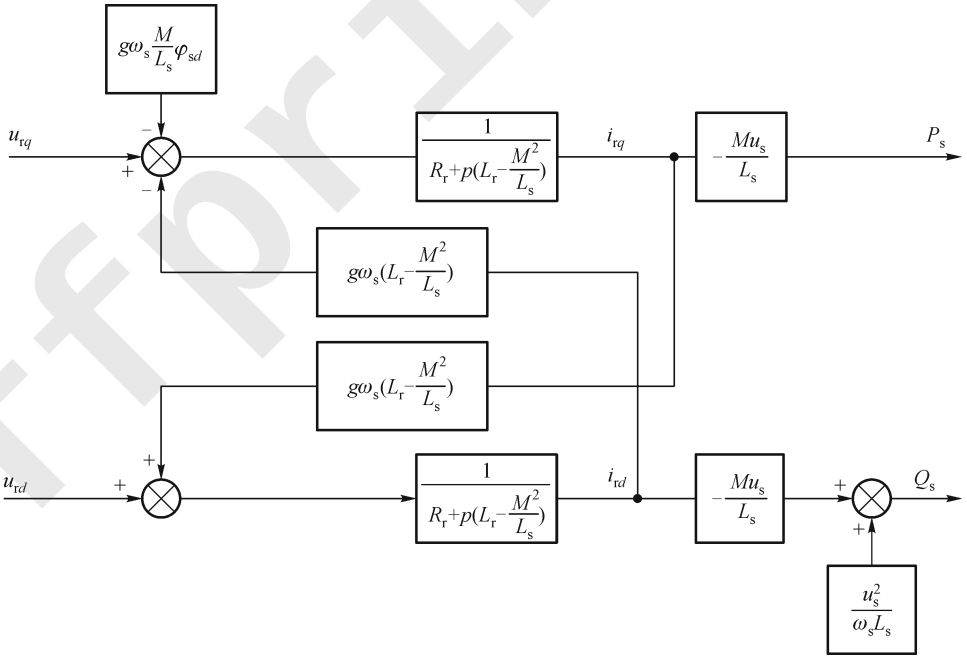

Fig. 5 Diagram of the machine

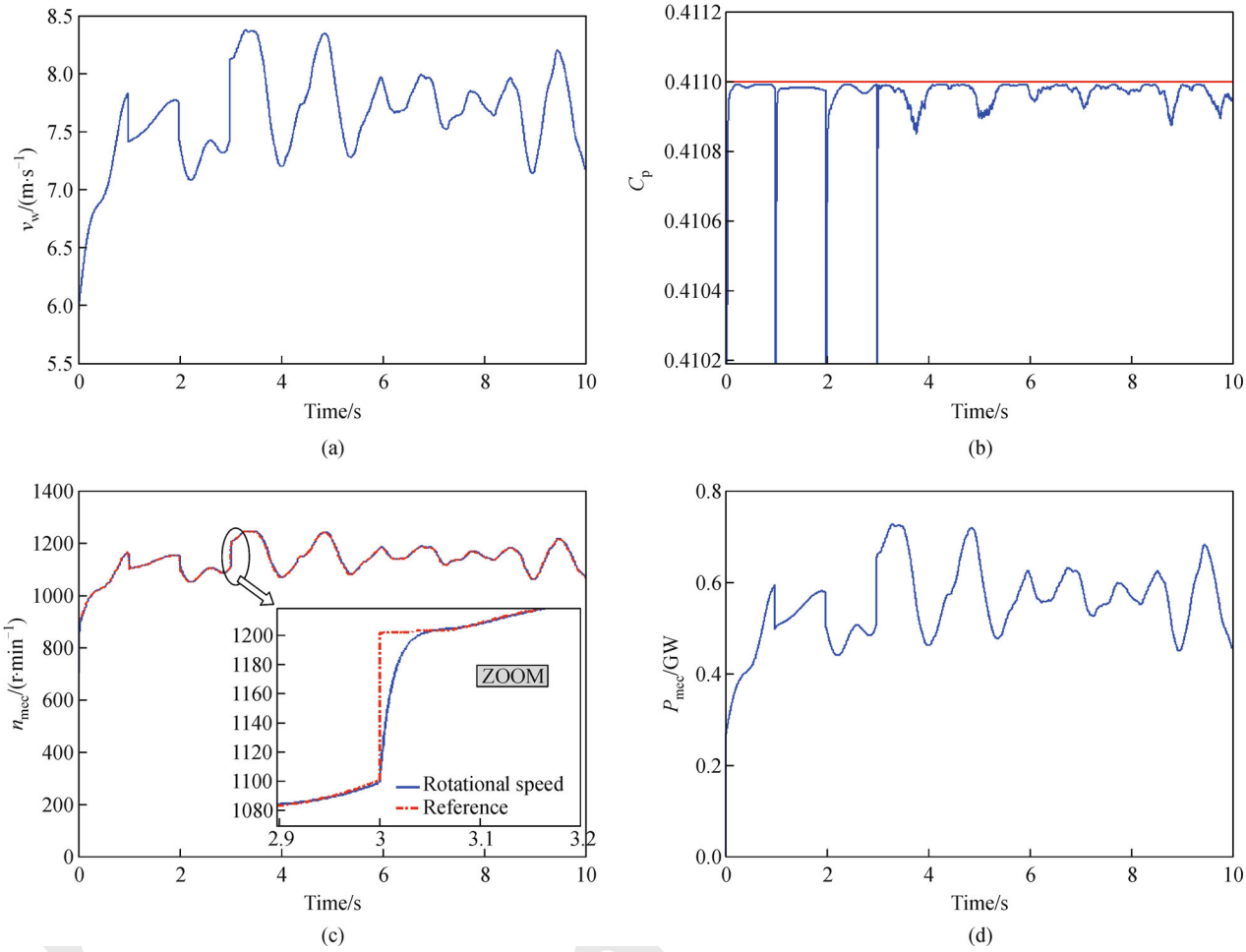

Fig. 7 Evolution of mechanical quantities of the wind turbine conversion
(a) Wind speed; (b) power coefficient; (c) angular speed of DFIG; (d) mechanical power of wind turbine

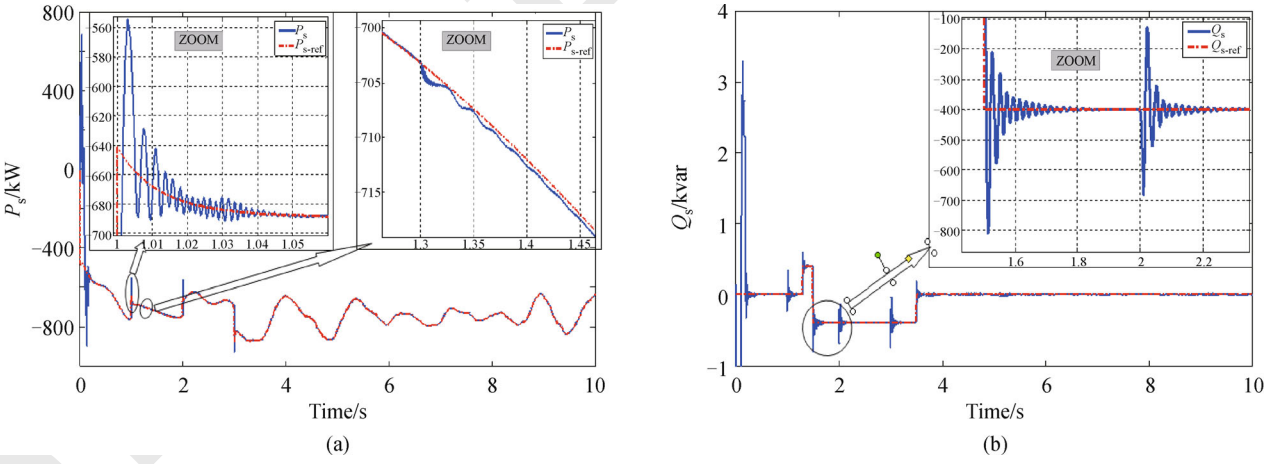

Fig. 8 Reference and measured active and reactive power
(a) Active power; (b) reactive power

As a first observation, the simulation results presented in Fig. 7 indicate that a small variation in the wind velocity can induce a large variation in the extracted power (mechanical power), because of the proportionality of

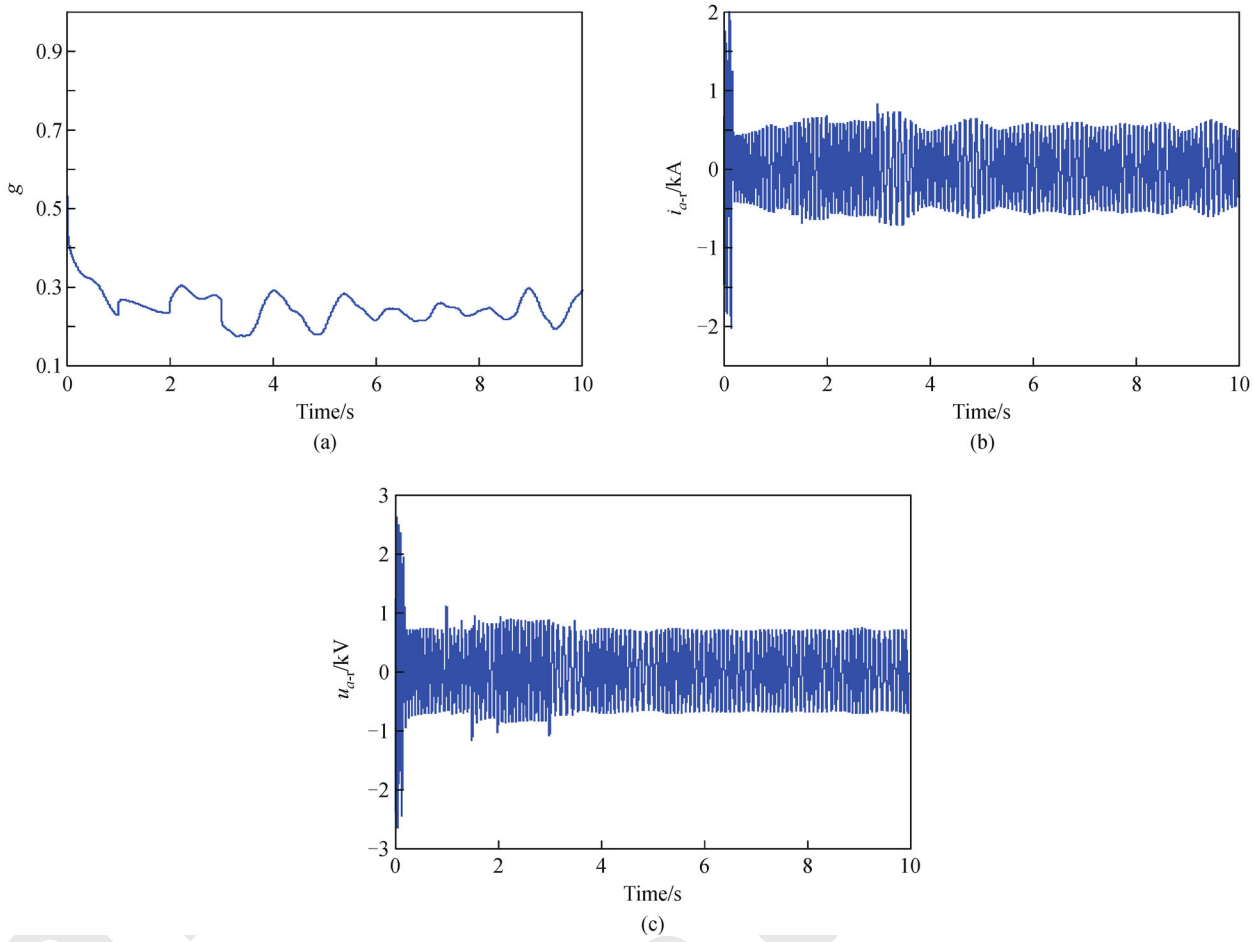

Fig. 9 Evolution of rotor currents and voltages following the slip
(a) DFIG slip; (b) rotor phase current; (c) rotor phase voltage of DFIG

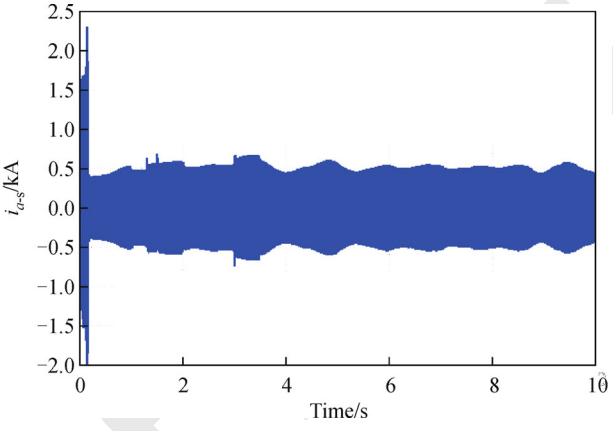

Fig. 10 DFIG stator current of a phase

this power to the average value of cubic wind speed.

It can be seen from Fig. 7(b) that the PI controller achieves a better speed tracking for maximum power generation, and then a better power extraction from the wind is achieved ($C_p \approx 0.41$).

From Fig. 8, it can be noticed that the stator active and reactive power flow in an acceptable way in accordance to their references at all time of the simulation. However, the effect of coupling between the active and reactive power can be observed, because a step on one of these two axes, or a variation on the second can lead to oscillations on the other. These oscillations appear apparently on the stator reactive power if a rapid change is made on the active power (at t = 1 s, at t = 2 s and at t = 3 s). Besides, the influence of variation of reactive power on the change of the error between the active power and its reference (for example at time t = 1.3 s) can also be noticed.

The current and voltage according to the rotor speed changes are given in Fig. 9. From Fig. 9, it can be seen that the electric frequency of the rotor variable varies with the rotor speed.

Globally, it can be found that most mechanical or electrical variables are related to the wind speed.

6.2 Second case of simulation (Robustness test of the control against the wind speed)

The robustness can be tested against external disturbances

such as speed and density of the wind or the fluctuation of frequency on the network. It can also be tested against the changing characteristics of the turbine. To test the robustness of the control against the wind speed, the behavior of the system is studied using three different wind profiles (v_{w1}, v_{w2} and v_{w3}). For each simulation test, the turbine starts in a different gust, approximately 4.5 m/s, 6 m/s, and 8 m/s.

Under different wind speed profiles, the simulation results of the active power according the MPPT and its zoom are shown in Fig. 11.

By comparing the results obtained for the three wind

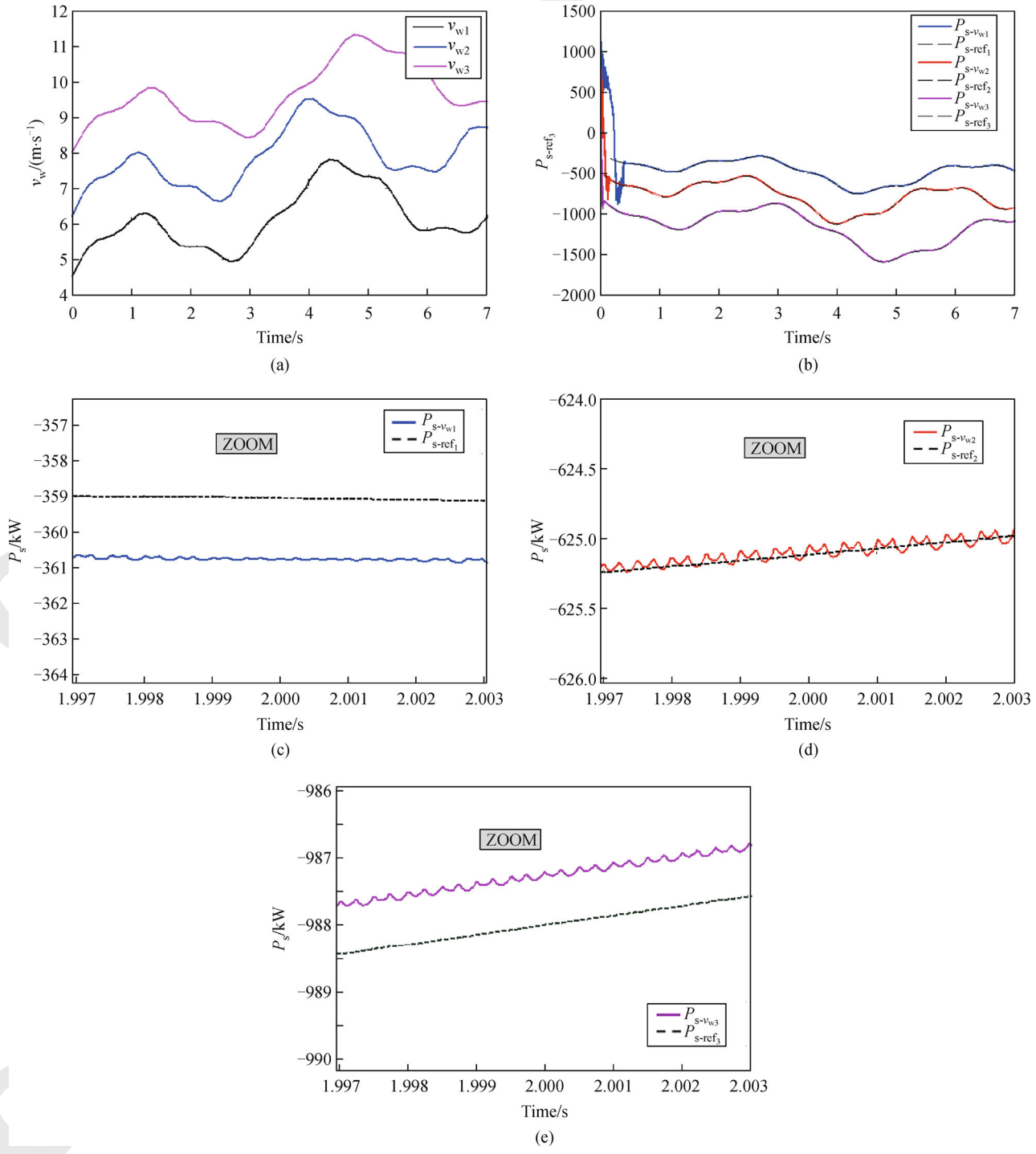

Fig. 11 System response for the three profiles of the wind

(a) Wind profiles; (b) simulation results of stator output active power for three profiles of the wind; (c) zoom of active power for the first profile of the wind; (d) zoom of active power for the second profile of the wind;(e) zoom of active power for the third profile of the wind

profiles, it can be seen that the response for active power increases at low starting wind speeds. It can also be seen that the active power has a lower error in the case where the turbine starts in a gust of approximately 6 m/s, (v_{w1}), and this error increases with the two other cases of wind profiles (v_{w2} and v_{w3}). The error between the active power and its reference appears apparently in the test results by changing the wind velocity; this makes it possible to highlight a remarkable degradation of the performance of the PI control.

7 Conclusions

The aim of this paper is to study a system which converts wind energy into electrical energy. In this paper, the overall system is represented, a classical PI mode vector control for a DFIG drive is used in order to control the output variables which are the stator active and reactive power of the DFIG injected in the grid, and a variable speed control of wind turbines is studied in order to maximize energy extraction from the wind. Simulation studies are conducted to verify the performance of the proposed PI controller under random wind fluctuations and variations of reactive power. It is noted the influence of the change in the wind speed at control power can reduce system performance. The proposed controller does not provide high-performance dynamic characteristics. On the one hand, this scheme is not perfectly robust against wind variations; on the other hand, it is preferable to estimate instead of measuring the speed, because the measurement of wind speed is generally not accurate.

References

1. Chitti Babu B, Monanty K B, Poongothai C. Performance of Double-Output Induction Generator for Wind Energy Conversion Systems. In: The First IEEE International Conference on Emerging Trends in Engineering and Technology. Nagpur, India, 2008, 933–938
2. Deepika K K, Srinivasa Rao A. Transient analysis of wind-based doubly-fed induction generator. International Journal of Engineering Research and Applications, 2012, 2(5): 524–527
3. Mohamed M, Hatoum A, Bouaouiche T. Flicker mitigation in a doubly fed induction generator wind turbine system. Mathematics and Computers in Simulation, 2010, 81(2): 433–445
4. El-Sattar A A, Saad N H, El-Dein M Z S. Dynamic response of doubly fed induction generator variable speed wind turbine under fault. Electric Power Systems Research, 2008, 78(7): 1240–1246
5. Yang L, Yang G Y, Xu Z, Dong Z Y, Wong K P, Ma X. Optimal controller design of a wind turbine with doubly fed induction generator for small signal stability enhancement. IET Generation, Transmission & Distribution, 2010, 4(5): 579–597
6. Wang S H, Chen S H. Blade number effect for a ducted wind turbine. Journal of Mechanical Science and Technology, 2008, 22 (10): 1984–1992
7. Serhoud H, Benattous D. Simulation of grid connection and maximum power point tracking control of brushless doubly-fed generator in wind power system. Frontiers in Energy, 2013, 7(3): 380–387
8. Poza J, Oyarbide E, Roye D. New vector control algorithm for brushless doubly-fed machines. In: IEEE 28th Annual Conference of the Industrial Electronics Society, 2002, 2: 1138–1143
9. Shao S Y, Abdi E, Barati F, McMahon R. Stator-flux-oriented vector for brushless doubly fed induction generator. IEEE Transactions on Industrial Electronics, 2009, 56(10): 4220–4228
10. Boyette A, Saadate S, Poure P. Direct and indirect control of a doubly fed induction generator wind turbine including a storage unit. In: Proceedings of IEEE 32nd Annual Conference on Industrial Electronics. Paris, France, 2006, 2517–2522
11. Egea-Alvarez A, Junyent-Ferré A, Gomis-Bellmunt O. Active and reactive power control of grid connected distributed generation systems. Modeling and Control of Sustainable Power Systems Green Energy and Technology, 2012, 47–81
12. Aktarujjaman M D, Kashem M A, Negnevitsky M, Ledwich G F. Smoothing output power of a doubly fed wind turbine with an energy storage system. In: Proceedings of Australian Universities Power Engineering Conference. Melbourne, Australia, 2006
13. Kassem A M, Hasaneen K M, Yousef A M. Dynamic modeling and robust power control of DFIG driven by wind turbine at infinite grid. International Journal of Electrical Power and Energy Systems, 2013, 44(1): 375–382
14. Yamamoto M, Motoyoshi O. Active and reactive power control for doubly-fed wound rotor induction generator. IEEE Transactions on Power Electronics, 1991, 6(4): 624–629
15. Poitiers F, Bouaouiche T, Machmoum M. Advanced control of a doubly-fed induction generator for wind energy conversion. Electric Power Systems Research, 2009, 79(7): 1085–1096